

## Time-resolved scanning Kerr microscopy of flux beam formation in hard disk write heads

Robert A. J. Valkass,<sup>1, a)</sup> Timothy M. Spicer,<sup>1</sup> Erick Burgos Parra,<sup>1</sup> Robert J. Hicken,<sup>1</sup> Muhammad A. Bashir,<sup>2</sup> Mark A. Gubbins,<sup>2</sup> Peter J. Czoschke,<sup>3</sup> and Radek Lopusnik<sup>3</sup>

<sup>1)</sup>*Department of Physics and Astronomy, University of Exeter, Stocker Road, Exeter, EX4 4QL, United Kingdom*

<sup>2)</sup>*Research & Development, Seagate Technology, 1 Disc Drive, Springtown Industrial Estate, Derry, BT48 0BF, United Kingdom*

<sup>3)</sup>*Recording Heads Operation, Seagate Technology, 7801 Computer Avenue South, Bloomington, Minnesota 55435, USA*

(Dated: 2 June 2016)

To meet growing data storage needs, the density of data stored on hard disk drives must increase. In pursuit of this aim the magnetodynamics of the hard disk write head must be characterized and understood, particularly the process of “flux beaming”. In this study, seven different configurations of perpendicular magnetic recording (PMR) write heads were imaged using time-resolved scanning Kerr microscopy, revealing their detailed dynamic magnetic state during the write process. It was found that the precise position and number of driving coils can significantly alter the formation of flux beams during the write process. These results are applicable to the design and understanding of current PMR and next-generation heat-assisted magnetic recording (HAMR) devices, as well as being relevant to other magnetic devices.

---

<sup>a)</sup>Corresponding author. [rajv202@ex.ac.uk](mailto:rajv202@ex.ac.uk)

## I. INTRODUCTION

Global data storage needs are currently estimated to be in the region of several hundred exabytes ( $10^{20}$  bytes) and only set to increase.<sup>1</sup> To meet these needs it is necessary to both improve the areal density of data storage devices and reduce the cost per gigabyte of storage.<sup>2</sup> In pursuit of these goals there are a number of potential areas for optimization, focused on enhancing the write head field while maintaining a consistent rise time and spatial confinement of the field. Achieving this not only leads to an increase in areal density, but also reduced write times and reductions in erase after write errors<sup>3</sup> and popcorn noise.<sup>4</sup>

The write heads studied here are effectively a planar electromagnet driven by electrically-conductive coils embedded beneath the magnetic material of the yoke. The write head is designed to maximize the available write field while minimizing erase after write errors and wide area track erasure.<sup>5</sup> It was first suggested by Mallery in 1985 that magnetic flux was conducted through structures similar to hard disk write heads by a process of small angle rotation of the magnetization, rather than by domain wall motion.<sup>6</sup> This leads to the formation of a narrow “beam” of flux along the central symmetry axis of the write head, a highly desirable property for generating both the strongest and most spatially uniform write field at the pole tip.

The presence of flux beams in similar write head structures has been observed before by time-resolved scanning Kerr microscopy (TRSKM).<sup>7</sup> These flux beams were also observed to form along the writer’s symmetry axis towards the pole tip. Furthermore, the equilibrium state of these writers has been inferred from TRSKM measurements<sup>8</sup> and later directly observed by x-ray photoemission electron microscopy.<sup>9</sup> However, time-resolved imagery of flux beams has only been recorded at a resolution of  $\approx 0.5$  ns. Little attention has been paid to the precise nature of the process of formation of these flux beams on the leading edge of the waveform, nor to the spatial character of the flux beams during the write process. This characterization is necessary to understand both the processes underpinning the formation of flux beams and how to develop write heads with robust flux beams that are more uniform and hence intense.

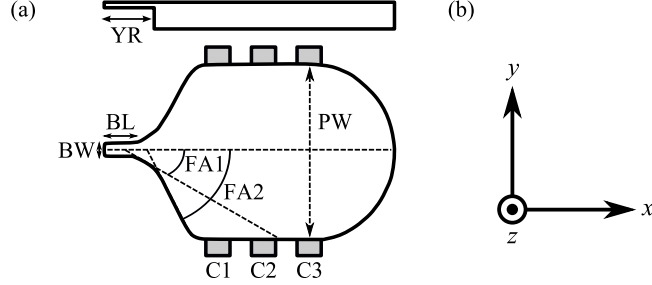


FIG. 1. (a) Schematic of a typical write head design, showing the geometric parameters used to define its shape. The configuration of active embedded driving coils C1–3 (shaded) varied between write heads. (b) The coordinate system used throughout the presented measurements.

## II. METHOD

The sample under investigation comprised a  $17 \times 15 \text{ mm}^2$  wafer piece containing a number of different geometric and electrical configurations of write heads. Each write head was fabricated from four repeats of a NiFe (1 nm)/CoFe (50 nm) bilayer chosen for its high magnetic moment and low coercive field. The shape of the write heads, shown in Fig. 1(a), was the same for all devices studied here. Write heads were of the typical “paddle” shape, with an overall paddle width (PW) of  $6.485 \mu\text{m}$  and confluence region flare angles (FA1 and FA2) of  $30^\circ$  and  $62^\circ$  respectively. The bridge measured  $1 \mu\text{m} \times 0.4 \mu\text{m}$  and the yoke was recessed by  $1.6 \mu\text{m}$ .

To emulate the formation of the flux beam during the data writing process, an electrical pulse was delivered through the coils embedded beneath the center part of the yoke inciting the magnetization to rotate. The coils were embedded  $500 \text{ nm}$  beneath the yoke, with each coil having a cross-section measuring  $1.5 \mu\text{m} \times 1 \mu\text{m}$  and intercoil spacing  $\approx 1 \mu\text{m}$ . The number and position of the active coils varied between write heads and is summarized in Table I. The electrical pulse was the same for all write heads, having an amplitude of  $4.7 \text{ V}$  and  $87.0 \text{ ps}$  duration (FWHM). The temporal form of the pulse can be seen in Fig. 2(b).

Changes to the magnetization were imaged using TRSKM, which has previously been described in detail.<sup>10–13</sup> A schematic of the experimental setup is shown in Fig. 2(a). An  $800 \text{ nm}$  wavelength Ti:sapphire ultrafast pulsed laser with  $80 \text{ MHz}$  repetition rate was used to make the measurements. The laser output was passed along a variable length optical delay line, providing time resolution to the measurements. The beam was then expanded

and clipped to improve uniformity before being polarized and delivered to the sample surface through a microscope objective lens with a numerical aperture of 0.85. This gave a diffraction-limited spot on the sample surface of diameter  $\approx 600$  nm.

Light reflected from the sample surface was then collected back through the same microscope objective and passed to a quadrant photodiode bridge detector<sup>14</sup> and lock-in amplifiers. This allowed simultaneous measurement of changes to the magnetization along the three mutually perpendicular spatial axes. Images were recorded at time intervals of  $\approx 10$  ps so as to explore the process of formation of a flux beam during the rise of the driving current.

### III. RESULTS

Figure 1 shows a schematic of the write head design and shared geometric parameters, as well as the coordinate system defined for these measurements. The three driving coils can be seen emerging from the sides of the structure. Kerr images of the seven write heads are shown in Figs. 3–9. For each device, the presented images have been selected for time delays at which changes are most noticeable<sup>15</sup>. A write head with all three driving coils connected, shown in Fig. 3, is expected to produce a uniform beam of flux along the central symmetry axis of the write head due to the uniformity of the driving field created by the coils. However, it was observed that flux through the yoke’s cross-section in fact nucleates in two smaller spots: one deep within the flared confluence region, and a second further

TABLE I. The driving coil configuration for each of the devices studied here, defined with reference to Fig. 1(a), where X denotes an active coil and — denotes an inactive coil.

Write head	Coil 1	Coil 2	Coil 3
F3	X	X	X
F5	X	—	—
F6	—	X	—
F7	—	—	X
F8	X	X	—
F9	X	—	X
F10	—	X	X

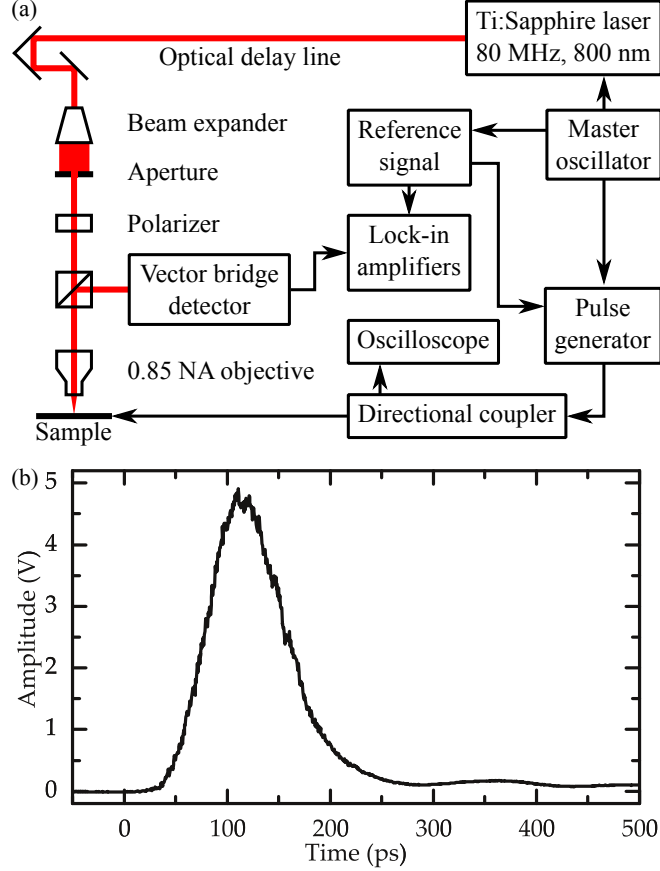


FIG. 2. (a) The time-resolved scanning Kerr microscope used for measurements of magnetization dynamics. A vector bridge detector allows for simultaneous detection of the three spatially perpendicular components of the magnetization.<sup>14</sup> (b) The temporal form of the driving pulse used to emulate the data writing process. The pulse had an amplitude of 4.7 V, full-width half-maximum duration of 87.0 ps and 10–90 rise time of 48.5 ps. The driving pulse repetition rate matched that of the laser.

towards the back via. While both of these areas of magnetic activity are located on the symmetry axis, they do not coalesce and no flux beam is formed.

Three of the write heads have only a single driving coil connected, however the spatial form of the flux beam varies greatly between these three structures. The first device (Fig. 4), having only coil C1 connected, shows a wide, uniform flux beam extending along the write head's symmetry axis. When only the central coil, C2, is connected two distinct narrow flux beams are formed either side of the symmetry axis, as shown in Fig. 5 (4.29 ns). With only C3 connected a uniform flux beam is formed along the symmetry axis, with outlying areas

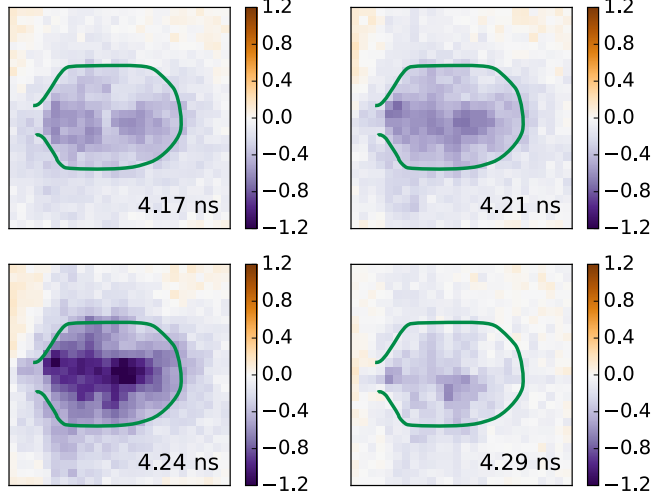


FIG. 3. Kerr images of write head F3 (coils C1, C2 and C3 active). Contrast shows changes to magnetization in the  $x$  direction,  $\Delta M_x$ , with negative values (purple) representing rotation to the left and positive values (orange) rotation to the right. The green outline is taken from a reflectivity image acquired simultaneously with the magnetic image, and is provided as a guide for the eye. Flux nucleates in two spots along the symmetry axis: one deep in the flared confluence region and one towards the back via. These distinct sites neither coalesce nor propagate, and no flux beam is formed.

of flux influencing the shape of the primary flux beam. This beam extends deep into the confluence region along the symmetry axis (Fig. 6).

Three of the write heads have two coils connected in various configurations. With the two coils closest to the confluence region connected (coils C1 and C2, Fig. 7) flux nucleates in two separate sites, before joining and extending along the symmetry axis of the write head. In contrast, the write head with two coils towards the back via activated (coils C2 and C3, Fig. 8) a disjointed flux beam is initially formed along the symmetry axis (4.37 ns), but rapidly breaks apart into a number of smaller sites (4.42 ns): one in the confluence region, one above the back via and a smaller area of contrast in the lower right of the image. Two spatially separated coils (C1 and C3, Fig. 9) lead to the development of a very broad, incoherent flux beam concentrated in the lower half of the writer with no evidence of further magnetization rotation towards the pole tip.

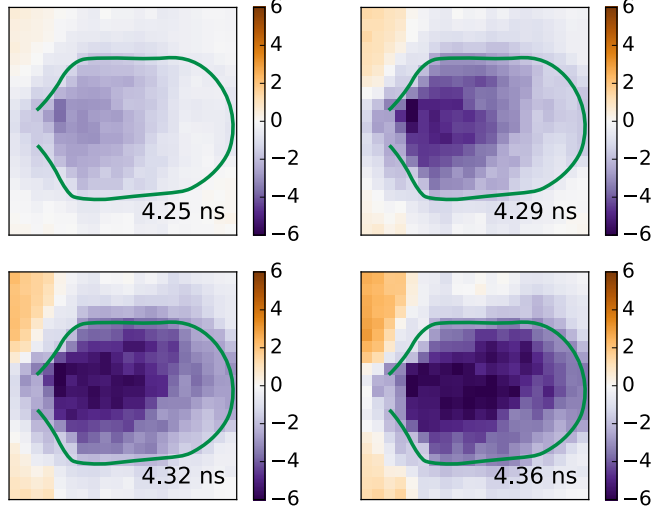


FIG. 4. Kerr images of write head F5 (coil C1 active). Contrast shows changes to magnetization in the  $x$  direction,  $\Delta M_x$ , with negative values (purple) representing rotation to the left and positive values (orange) rotation to the right. The green outline is taken from a reflectivity image acquired simultaneously with the magnetic image, and is provided as a guide for the eye. A very broad area of magnetization rotation is observed, extending along the symmetry axis.

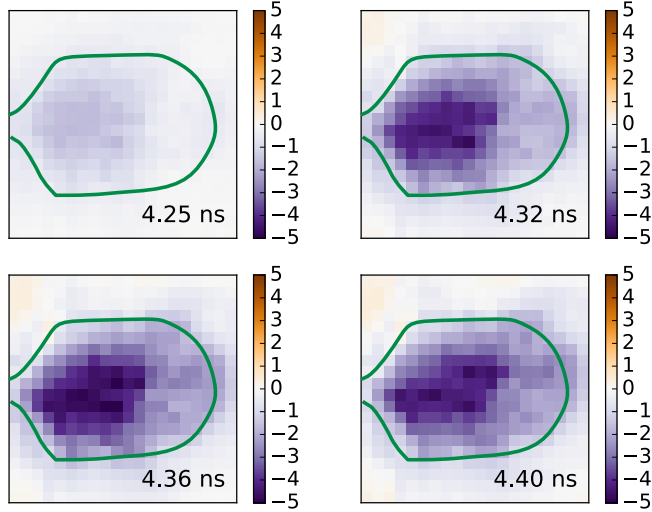


FIG. 5. Kerr images of write head F6 (coil C2 active). Contrast shows changes to magnetization in the  $x$  direction,  $\Delta M_x$ , with negative values (purple) representing rotation to the left and positive values (orange) rotation to the right. The green outline is taken from a reflectivity image acquired simultaneously with the magnetic image, and is provided as a guide for the eye. Two narrow flux beams are formed, one either side of the symmetry axis.

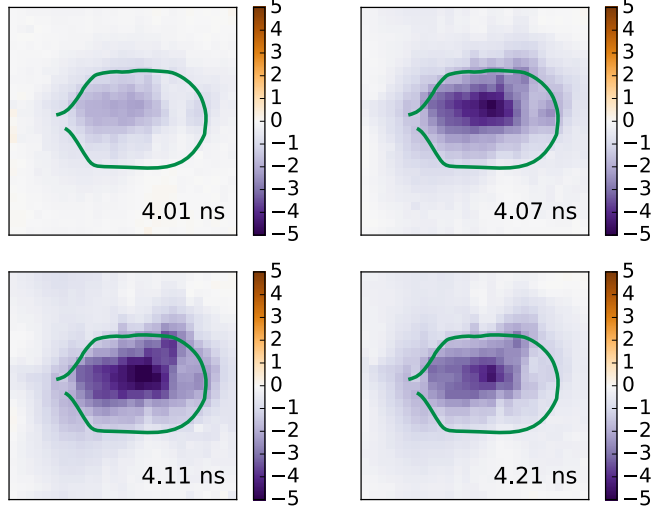


FIG. 6. Kerr images of write head F7 (coil C3 active). Contrast shows changes to magnetization in the  $x$  direction,  $\Delta M_x$ , with negative values (purple) representing rotation to the left and positive values (orange) rotation to the right. The green outline is taken from a reflectivity image acquired simultaneously with the magnetic image, and is provided as a guide for the eye. A relatively uniform flux beam is formed along the symmetry axis, extending into the confluence region.

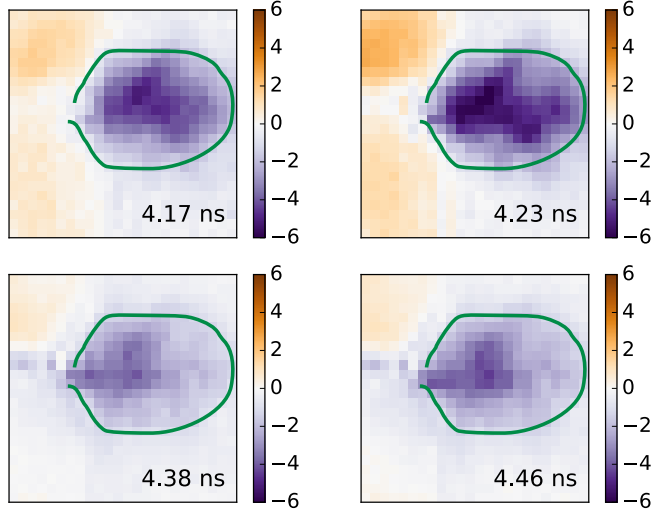


FIG. 7. Kerr images of write head F8 (coils C1 and C2 active). Contrast shows changes to magnetization in the  $x$  direction,  $\Delta M_x$ , with negative values (purple) representing rotation to the left and positive values (orange) rotation to the right. The green outline is taken from a reflectivity image acquired simultaneously with the magnetic image, and is provided as a guide for the eye. Flux initially nucleates in a number of separate sites, before coalescing and extending along the symmetry axis.



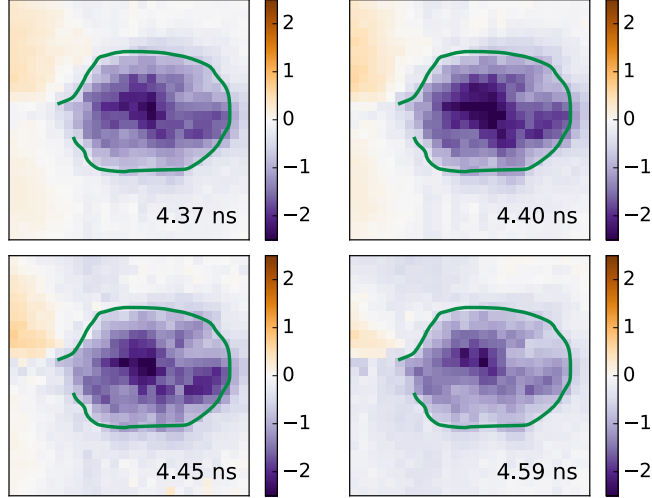


FIG. 8. Kerr images of write head F10 (coils C2 and C3 active). Contrast shows changes to magnetization in the  $x$  direction,  $\Delta M_x$ , with negative values (purple) representing rotation to the left and positive values (orange) rotation to the right. The green outline is taken from a reflectivity image acquired simultaneously with the magnetic image, and is provided as a guide for the eye. A disjointed flux beam is seen to form at 4.37 ns, but this rapidly breaks apart instead of propagating.

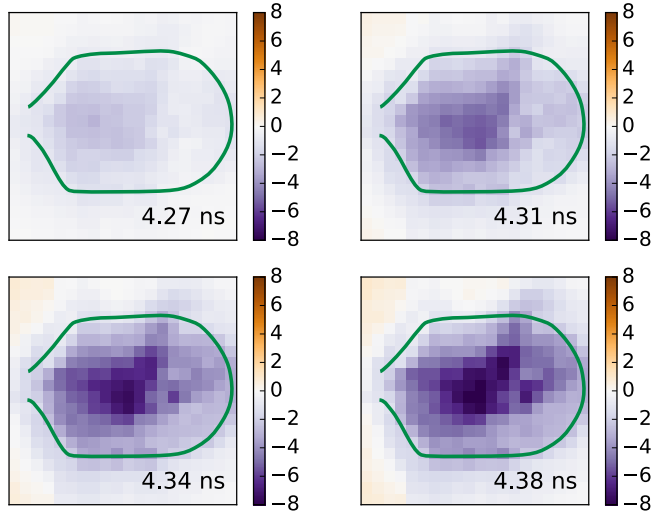


FIG. 9. Kerr images of write head F9 (coils C1 and C3 active). Contrast shows changes to magnetization in the  $x$  direction,  $\Delta M_x$ , with negative values (purple) representing rotation to the left and positive values (orange) rotation to the right. The green outline is taken from a reflectivity image acquired simultaneously with the magnetic image, and is provided as a guide for the eye. A broad flux beam is formed in the yoke, with no evidence of magnetization rotation in the pole tip.

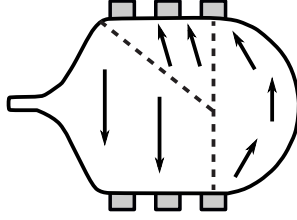


FIG. 10. The equilibrium state of a write head nominally identical to those presented here has been reported previously.<sup>9</sup> This domain structure can be considered indicative of the structure of similar devices.

#### IV. ANALYSIS OF OBSERVED FLUX FORMATIONS

An equilibrium magnetic state for nominally identical devices of this shape has been reported previously,<sup>9</sup> and is reproduced in Fig. 10. Three primary domains comprise the equilibrium state. The largest is oriented in the parallel direction (along the easy axis of the structure) and occupies the confluence region and lower half of the write head. A smaller domain occupies the upper half of the write head and a third domain covers the back via, with the magnetization orienting itself to satisfy the shape anisotropy in this region.

With all three write coils activated, as in device F3, the formation of a strong, uniform flux beam directly along the write head’s symmetry axis is expected. Instead, flux is observed nucleating in two spatially separated spots along the symmetry axis. This is likely due to the equilibrium state’s deviation from the theorized “striped” domain state.<sup>16</sup> The fragmented nature of the flux beam suggests instead the presence of regions where the magnetization is canted from the parallel direction and so undergoes smaller rotation in response to the field from the coils.

In the case of write heads with a single active driving coil the observed behaviour is much as expected. With a single active coil, it is expected that flux would nucleate above the coil, and propagate along the symmetry axis by means of a process of small-angle domain rotation, without the need for motion of domain walls.<sup>6</sup> For two of the single-coil write heads, F5 and F7, this behaviour is indeed observed; flux nucleates in a single location above the driving coil before extending along the symmetry axis towards the pole tip. It is possible that the magnitude of the in-plane field must exceed a threshold value to cause rotation of the magnetization from the equilibrium state. This would occur first above the driving coil, before rotation would be observed at greater distances from the coil. Unfortunately

the spatial resolution limit of optical Kerr microscopy prevents observation of the detailed magnetic structure within the pole tip during the writing process.

The write head with only the single central driving coil activated (write head F6), however, does not exhibit this expected behaviour. Flux nucleates in two spatially separated areas above the driving coil, either side of the symmetry axis. These then extend independently towards the pole tip, and remain spatially separated. The line separating the two regions of flux might be associated with the presence of a domain wall since a diagonal domain wall has been observed previously in similar devices (Fig. 10). It is possible that an alternative equilibrium domain structure would lead to more favorable conditions for flux beaming.

Two neighbouring active coils, as is the configuration in write heads F8 and F10, should exhibit similar behaviour to their single-coil equivalents. The two coils should produce a region of in-plane field of larger area, nucleating a larger area of flux, hence producing a broader flux beam. However, this is not the observed behavior in either of these write heads.

The two coils closest to the pole tip (coils C1 and C2) nucleate two distinct areas of flux: one in the lower half of the yoke, and a second above the back via. The nucleation of flux above the back via is surprising given the distance from the driving coils. This may suggest movement of a domain wall, contrasting with predictions that flux propagation is the result only of small-angle magnetization rotation within existing domains. The two distinct areas of flux do, however, then coalesce so as to extend along the symmetry axis towards the pole tip.

Conversely, the two coils towards the back of the writer (coils C2 and C3) nucleate a number of small areas of flux covering most of the yoke. These areas of flux dissipate rather than coalescing, and fail to form a continuous flux beam. The image at 4.59 ns shows more structure, with a very wide beam covering most of the yoke, and a region of strong contrast above coil C3. This area may align with a domain wall at the back of the device and perpendicular to the symmetry axis, suggesting that once again the domain wall plays a role in disrupting the formation of a flux beam within the yoke.

Two spatially separated coils, one deep in the confluence region and the second towards the back via (coils C1 and C3), produce a broad, incoherent flux beam which fails to extend along the symmetry axis. There are two potential explanations for this behaviour. Firstly, the polar field between the two active coils varies more strongly due to their increased spatial

separation. Alternatively this writer may have a slightly different equilibrium state to that expected, perhaps moving the rear domain wall being located closer to coil C2.

The apparent role of domain walls in determining the success (or otherwise) of flux beaming in a writer suggests the equilibrium state of the writer is of crucial importance in determining the exact nature of the flux beam formation.

The ultimate aim of these write head structures is twofold. First, to achieve the highest possible data transfer rate through fast switching of both the write head and the underlying magnetic storage medium. Secondly, to shrink magnetic storage systems and increase data storage density by increasing the spatial confinement of the write field. While the simplest and most obvious method to increase the write field would be to increase the saturation flux density of the head material, this has previously been shown to be insufficient to obtain desired increases in recording field strength.<sup>17</sup> This increase has therefore conventionally been achieved by increasing the number and density of the driving coils, increasing the driving current and adjusting the geometry of the write head. However, the time-resolved images obtained from this range of coil configurations show a surprisingly large variation in the precise spatial form of the nucleated flux within the yoke and confluence region. This implies particular attention must be paid to the exact micromagnetic state of the writer.

These results do, however, suggest a potentially preferable configuration for the driving coils. A single driving coil positioned close to the air-bearing surface, driven with sufficiently high current to cause the pole tip magnetization to rotate parallel to the symmetry axis, would likely produce a wide but uniform propagating flux beam similar to that observed in device F5 (Fig. 4(a)). A reduction in the number of driving coils would also assist scaling of the yoke and pole tip to smaller dimensions and would reduce the self-inductance of the coil promoting reduced switching times.

## V. CONCLUSIONS

We have demonstrated that the detailed spatial form of the driving field, generated by the embedded write coils, plays a significant role in the magnetodynamics observed within commercial hard disk write heads. However, the considerable variation in observed dynamics further suggest that the equilibrium state plays an equally important role.

We have also provided experimental observations of the process of flux beaming. While

current models for flux conduction<sup>6</sup> sufficiently describe the fundamentals of the process, refinement is required to replicate the magnetic processes observed in real-world devices with complex geometry. Furthermore, the term “flux beaming” appears to be somewhat of a misnomer: dynamic flux rarely forms uniform “beams”, nor does flux propagate on the picosecond timescale and 600 nm resolution presented here.

This work has immediate application in understanding the magnetodynamics of hard disk write heads and other high-frequency nanoscale magnetic devices. This also provides insight for future write head designs, particularly for heat-assisted magnetic recording (HAMR) devices, ultimately leading to greater areal density and cheaper magnetic storage.

## SUPPLEMENTARY MATERIAL

See supplementary material for the complete set of images for all the devices presented here.

## ACKNOWLEDGMENTS

The authors gratefully acknowledge financial support from the Seagate Plan.

The underlying research dataset supporting this publication is available under a Creative Commons Attribution-ShareAlike 4.0 International License (<https://creativecommons.org/licenses/by-sa/4.0/>) and can be publicly accessed in Open Research Exeter via the following persistent identifier: <http://hdl.handle.net/10871/21108>.

## REFERENCES

- <sup>1</sup>S. Iwasaki, *Journal of Magnetism and Magnetic Materials* **324**, 244 (2012).
- <sup>2</sup>R. E. Fontana, S. R. Hetzler, and G. Decad, *IEEE Transactions on Magnetics* **48**, 1692 (2012).
- <sup>3</sup>M. S. Patwari and R. H. Victora, *IEEE Transactions on Magnetics* **46**, 1212 (2010).
- <sup>4</sup>F. H. Liu and M. H. Kryder, *Journal of Applied Physics* **75**, 6391 (1994).
- <sup>5</sup>H. J. Richter, *Journal of Physics D: Applied Physics* **40**, R149 (2007).
- <sup>6</sup>M. L. Mallery, *Journal of Applied Physics* **57**, 3952 (1985).

- <sup>7</sup>P. Gangmei, P. S. Keatley, W. Yu, R. J. Hicken, M. A. Gubbins, P. J. Czoschke, and R. Lopusnik, *Applied Physics Letters* **99**, 232503 (2011).
- <sup>8</sup>W. Yu, P. Gangmei, P. S. Keatley, R. J. Hicken, M. A. Gubbins, P. J. Czoschke, and R. Lopusnik, *Applied Physics Letters* **102**, 162407 (2013).
- <sup>9</sup>R. A. J. Valkass, W. Yu, L. R. Shelford, P. S. Keatley, T. H. J. Loughran, R. J. Hicken, S. A. Cavill, G. van der Laan, S. S. Dhesi, M. A. Bashir, M. A. Gubbins, P. J. Czoschke, and R. Lopusnik, *Applied Physics Letters* **106**, 232404 (2015).
- <sup>10</sup>M. R. Freeman and J. F. Smyth, *Journal of Applied Physics* **79**, 5898 (1996).
- <sup>11</sup>W. K. Hiebert, A. Stankiewicz, and M. R. Freeman, *Physical Review Letters* **79**, 1134 (1997).
- <sup>12</sup>A. Barman, V. V. Kruglyak, R. J. Hicken, A. Kundrotaite, and M. Rahman, *Applied Physics Letters* **82**, 3065 (2003).
- <sup>13</sup>A. Neudert, P. S. Keatley, V. V. Kruglyak, J. McCord, and R. J. Hicken, *IEEE Transactions on Magnetics* **44**, 3083 (2008).
- <sup>14</sup>W. W. Clegg, N. A. E. Heyes, E. W. Hill, and C. D. Wright, *Journal of Magnetism and Magnetic Materials* **95**, 49 (1991).
- <sup>15</sup>See supplementary material for the complete image sequences.
- <sup>16</sup>M. Mallery, “The physics of ultra-high-density magnetic recording,” (Springer Science+Business Media, Berlin, 2001) Chap. 11—Recording Head Design, pp. 314–348.
- <sup>17</sup>Y. Kanai, R. Matsubara, H. Watanabe, H. Muraoka, and Y. Nakamura, *IEEE Transactions on Magnetics* **39**, 1955 (2003).